

Autonomous Self-Healing UAV Swarms for Robust 6G Non-Terrestrial Networks

Sambrama Hegde*, Venkata Srirama Rohit Kantheti*, Liang C Chu†, Erik Blasch‡, and Shih-Chun Lin*

*North Carolina State University, Raleigh, NC, USA, {sambram, vkanthe, slin23}@ncsu.edu

†Lockheed Martin Space, Sunnyvale, CA, USA, liang.c.chu@lmco.com

‡Air Force Research Lab, Rome, NY, USA, erik.blasch.1@us.af.mil

Abstract—Recent years have seen an increased interest in the use of Non-terrestrial networks (NTNs), especially the unmanned aerial vehicles (UAVs) to provide cost-effective global connectivity in next-generation wireless networks. We introduce a resilient, adaptive, self-healing network design (RASHND) to optimize signal quality under dynamic interference and adversarial conditions. RASHND leverages inter-node communication and an intelligent algorithm selection process, incorporating combining techniques like distributed-Maximal Ratio Combining (d-MRC), distributed-Linear Minimum Mean Squared Error Estimation (d-LMMSE), and Selection Combining (SC). These algorithms are selected to improve performance by adapting to changing network conditions. To evaluate the effectiveness of the proposed RASHND solutions, a software-defined radio (SDR)-based hardware testbed afforded initial testing and evaluations. Additionally, we present results from UAV tests conducted on the AERPAW testbed to validate our solutions in real-world scenarios. The results demonstrate that RASHND significantly enhances the reliability and interference resilience of UAV networks, making them well-suited for critical communications.

Index Terms—Self-healing, device-to-device communication.

I. INTRODUCTION

Growing demand for high quality networks, driven by connected devices, automation, and smart cities, has increased the need for resilient networks. Adequate broadband coverage in remote and rural areas remains a challenge for existing wireless networks. Increasing cellular site density can improve network resilience but entails significant deployment, operational costs, and higher energy consumption. To address these challenges, NTNs have become a key focus of next-generation (next-G) communication systems. Next-G systems shift from traditional infrastructure to heterogeneous architectures, integrating terrestrial networks with NTNs, and satellites. These systems aim to offer on-demand and cost-effective coverage solutions across regions, thereby enabling seamless, ubiquitous, and high-capacity connectivity [1]–[4].

UAVs among NTNs offer high mobility and flexible deployment, providing connectivity to areas without infrastructure. They adapt as relays, flying base stations, or mobile edge computing nodes to boost coverage and computation, reaching hard-to-reach rural and isolated areas unlike fixed networks [5]. Moreover, UAVs can operate collaboratively in swarms to form Single-Input Multiple-Output (SIMO) or Multiple-Input

Multiple-Output (MIMO) systems, enabling spatial diversity and thus, improving signal quality. By leveraging diversity in swarm configurations, the impact of jammers can be minimized, improving the overall reliability of the network [6].

Self-healing is the ability of the system to detect and recover from abnormalities with minimal or no human intervention [7]. Self-healing network (SHNs) play an important role in complex environments like the ones involving UAVs, where having manual intervention is not feasible. SHNs help network function smoothly by handling issues including interference and node failures. A SHN intelligently switches between various combining techniques based on the condition. This ensures that the system is reliable and has high performance even in adverse conditions.

Inter-device links (IDL) are used to ensure reliable communication between the UAVs [8]. IDLs also enable key applications like swarm flight and collision avoidance, while improving spectral/energy efficiency, coverage, and reducing backhaul dependency [9]. IDLs allow UAVs to exchange data by establishing direct links and thus maintain reliable connections even in challenging environments. We develop the RASHND system with device-to-device (D2D) communication functionalities to mimic the characteristics of IDLs.

The proposed hardware end-to-end system is implemented using the Universal Software Radio Peripheral (USRP) B210s along with Raspberry Pi's (RPi) to enable self-healing on bit-stream and image data. The d-MRC and d-LMMSE algorithms used in self-healing along with the signal processing techniques used to process and extract the data have already been introduced in our previous work [6]. The wireless transmission of the extracted data among the RPis happens seamlessly through an internal ad-hoc network. AERPAW testbed is used to validate our results on UAV based testbed [10].

The remainder of the paper is divided as follows. Section II discusses the proposed RASHND system architecture and the indoor and outdoor hardware testbeds. Section III introduces the algorithms and the state machine used for our SHN. Section IV talks about inter-device links. We present the results in section V and finally conclude the paper in section VI.

II. SYSTEM ARCHITECTURE

This section presents the RASHND architecture, along with the hardware testbeds used to validate our algorithms.

This research work was supported by Lockheed Martin Space.

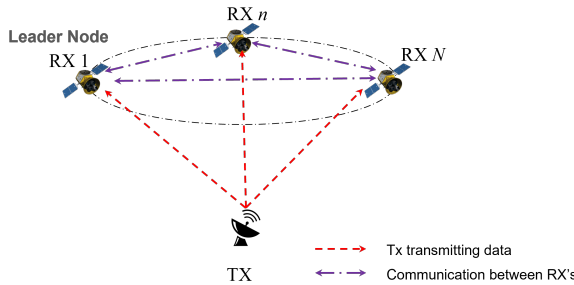


Fig. 1: Proposed RASHND architecture.

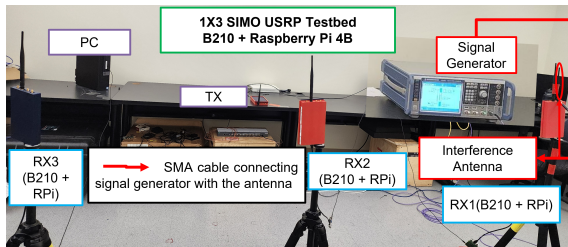


Fig. 2: Indoor testbed for 1×3 SIMO testbed.

A. Proposed Architectural Model

Fig. 1 illustrates the proposed system architecture, which consists of a SIMO setup with one transmitter (TX) and N receivers (RX). The TX is a ground terminal that continuously transmits signals to the swarm of receivers in the air. These RXs, part of a swarm system, connect via an internal ad-hoc network for D2D communication and coordination. The RASHND network allows each device to share locally processed signal data with the rest of the swarm. A designated leader node within the swarm is responsible for collecting the processed data from all RX units and applying the appropriate combining algorithm to enhance signal quality. To ensure robustness and avoid single points of failure, the leader node role is dynamically assigned to different RXs sequentially. In the example shown in Fig. 1, RX1 is the leader node for that instance, demonstrating the flexibility and distributed control of the system.

B. Experimental Testbed Setup

1) *Indoor Testbed*: Fig. 2 represents the testbed used to implement the system in an indoor setup. The setup includes three USRP B210s, each connected to a RPi, functioning as the RXs. An additional USRP B210 is connected to a PC and serves as the TX. The RPis control the RX units, and their compact, low-power design enables portable and flexible testing. An antenna connected to a signal generator is placed close to RX1 to introduce jamming into the system.

2) *Outdoor Testbed*: Fig. 3 represents the testbed used to implement the system in an outdoor environment. The setup includes five USRP B210s, each connected to a RPi, three of them functioning as RXs, with one each as TX and the jammer (JX). All our devices are placed on tripod stands and are distant from each other when compared to the indoor testbed.

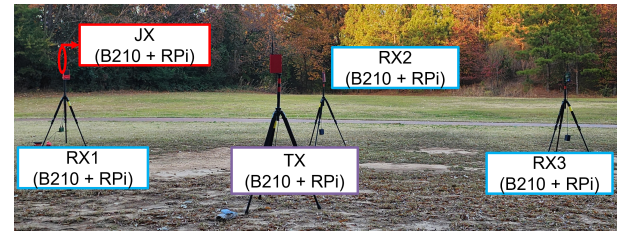


Fig. 3: Outdoor testbed for 1×3 SIMO testbed.

III. SELF-HEALING PROPOSAL

This section presents the algorithms included in our setup and the proposed self-healing network.

A. Algorithms Implemented in Self-Healing

RASHND transitions among three algorithms to achieve superior signal quality, which are briefly described here.

1) *Distributed Maximal Ratio Combining (d-MRC)*: The d-MRC algorithm combines data from multiple receivers weighted by channel quality [6].

The signal data at each of the RX can be written as,

$$\mathbf{r}_i[k] = \sqrt{p_g} h_i \mathbf{x}[k] + \sqrt{p_j} h_{j,i} \mathbf{x}_j[k] + \mathbf{n}_i, \quad (1)$$

where, p_g and p_j are the TX and JX power respectively, h_i and $h_{j,i}$ are SISO channel and the jammer channel information for the i th receiver, \mathbf{x} and \mathbf{x}_j are the input sequences for the TX and the JX respectively, and \mathbf{n}_i is the iid noise.

In accordance with Eq. (1), the data from all the receivers are collected into a single data structure for further processing. If there are a total of N receivers, then $\mathbf{R} = [r_1, r_2, \dots, r_N]^T$, represents this data structure. d-MRC exploits uncorrelated channels to combine signals that carry same information. d-MRC multiplies the data at all receivers with a weight vector $\mathbf{u} = [u_1, u_2, \dots, u_N]^T$, such that the effective signal-to-noise ratio (SNR) is maximized. The interference is assumed to be negligible and thus, $\sqrt{p_j} h_{j,i} \mathbf{x}_j[k]$ can be ignored. The SNR for the combined result can thus be written as,

$$\text{SNR} = \frac{p_g \sum_{(i=1)}^N \|u_i^H h_i\|^2}{\sigma^2 \sum_{(i=1)}^N \|u_i\|^2}, \quad (2)$$

where σ^2 is the Additive White Gaussian Noise (AWGN) noise power level, $\mathbf{h} = [h_1, h_2, \dots, h_N]^T$ represents a vector of channel state information from N receivers and $(\cdot)^H$ is the Hermitian operator.

By optimizing as in [11] and applying the Cauchy-Schwarz Inequality, we obtain the d-MRC weight \mathbf{u}_{d-MRC} as,

$$\mathbf{u}_{d-MRC} = \mathbf{h}^H. \quad (3)$$

2) *Distributed Linear Minimum Mean Square Error Estimation (d-LMMSE)*: The d-LMMSE algorithm uses a weighted combination of data, including interference, making it effective for signals with high interference such as jamming [6]. The

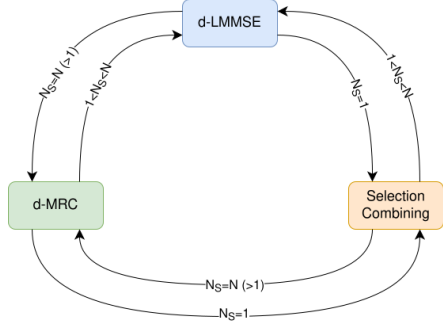


Fig. 4: State machine for self-healing.

effective signal-to-interference-plus-noise ratio (SINR) can be written as,

$$\text{SINR} = \frac{p_g \sum_{(i=1)}^N \|u_i^H h_i\|^2}{\sigma^2 \sum_{(i=1)}^N \|u_i^H\|^2 + p_j \sum_{(i=1)}^N \|u_i^H h_{j,i}\|^2}. \quad (4)$$

The optimal value of \mathbf{u} is found by maximizing SINR via the above equation as a minimum mean squared error problem. Assuming transmitted signals are legitimate, so that external interference and noise are independent, we obtain,

$$\mathbf{u}_{d-LMMSE} = p_g [p_g \mathbf{h} \mathbf{h}^H + p_j \mathbf{h}_j \mathbf{h}_j^H + \sigma^2 \mathbf{I}]^{-1} \mathbf{h}, \quad (5)$$

where, \mathbf{I} is the identity matrix of size $N \times N$.

3) *Selection Combining (SC)*: Selection Combining selects the best of the N receivers at any time [12]. Mathematically, this is similar to Eq. (2), where RXs heavily affected by interference have a weight vector of 0. This leaves the combined signal to be equal to the signal with legitimate data, thus making the weight vector for that particular RX to be 1.

B. State Machine Model for Self-Healing

Self-healing is implemented to make the system independent and have the best possible combining algorithm implemented at all times in order to obtain a superior quality signal. Fig. 4 represents the state machine used to implement the combining method. The SHN algorithm is selected based on the number of receivers, N_s , having bit error rates (BER) greater than the threshold. One among d-MRC, d-LMMSE and SC gets chosen based on the BER values.

Fig. 4 describes the implementation of the three combining algorithms. When all the RXs receive high quality signals, the BER for each of the RX units will be greater than the given threshold. Here, the number of receivers with BER greater than the threshold, N_s , will be equal to the total number of available receivers, i.e., $N_s = N$, prompting the system to implement d-MRC. In cases of extremely high interference, where only one of the RXs receive a good signal, i.e., $N_s = 1$, the system implements SC, where the best performing receiver is chosen. Another scenario is when the number of RXs receiving high quality signal is more than one but less than the total number of available receivers.

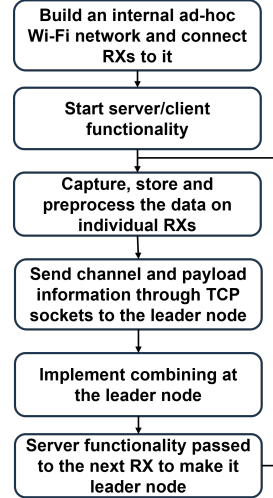


Fig. 5: Flow diagram for inter-device links.

IV. INTER-DEVICE LINKS

To develop a self-sufficient swarm system with IDL capabilities, we designed a network of RXs capable of direct D2D communication. Each RX shares data over a dedicated wireless channel, different from the SIMO communication channel. The RASHND architecture allows the RXs to perform signal combining locally, removing the need for an external computer and making the swarm system autonomous.

TCP sockets enable D2D communication, allowing each RX to act as both client and server. The flow diagram in Fig. 5 represents the system flow. Upon startup, all devices connect to a common Wi-Fi network using the onboard network interface cards on the RPis. Once connected, the RXs establish TCP server-client connections in a dynamic, rotating fashion [13]. Initially, RX1 acts as the server (leader), with other RXs as clients. After each processing cycle, the server role rotates to RX2, RX3, and so on, ensuring all devices take turns coordinating data exchange and processing.

During operation, each RX captures and processes its signal data, storing channel and payload information locally. Client RXs then transmit the processed data to the current leader node via established TCP sockets. The leader node computes each receiver's BER, compares it to a threshold, and selects the optimal combining algorithm. Once the combining process is complete, the leader node capabilities are passed to the next RX in the sequence, and the process repeats, enabling continuous and distributed operation without external oversight.

To enhance robustness, the RXs are programmed to automatically detect and recover from communication failures. If the connection is lost, the devices attempt to reconnect without requiring the system to restart. Should a particular RX become unavailable, the system simply excludes it from the combining process and continues operating with the remaining devices. This fault-tolerant design ensures the UAV swarm remains resilient and independent of any single node.

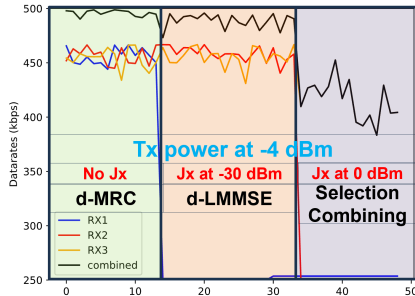


Fig. 6: Data rates for bitstream data for indoor testbed.

V. OVER THE AIR IMPLEMENTATION

This section discusses the results obtained for self-healing network in the indoor and outdoor testbed. We present the results for bitstream and image data, along with the results for UAV based testing using the AERPAW platform.

A. Self-Healing on Indoor Testbed

Our algorithms are at first validated in our indoor testbeds.

1) *Results for Bitstream Data:* The system is first tested for bitstream data, where a random set of data is generated and modulated using QPSK modulation and then, appended with Zadoff-Chu preamble sequence. We use a center frequency of 2.55 GHz, a bandwidth of 1 MHz and RX power of -49 dBm. The data is continuously transmitted at a constant power of -4 dBm. The entire reception is automated to work with self-healing. Each B210 captures the data, which the RPi stores and compensates for timing, frequency and phase difference, determines the channel estimates and the payload information. The channel estimates and payload information are shared with the leader node through D2D communication to implement the combining algorithm and obtain the data rates.

Fig. 6 represents the continuous plot for bitstream data through self-healing implemented using the automated setup. With no interference, all three receivers achieve high data rates, showing that the d-MRC algorithm is applied since their BERs exceed the threshold. We then introduce -30 dBm external interference. The receiver nearest to the interference antenna, RX1, is affected, so d-LMMSE is applied. Further increasing the interference power to 0 dBm impacts both RX1 and RX2. Thus, SC is implemented, and the combined data rate equals the best performing receiver, RX3.

2) *Results for Image Data:* Since self-healing works well on bitstream data, it is extended to larger datasets like images. A small airplane image is converted to grayscale and vectorized, then turned into bitstream for transmission, similar to previous bitstream data. The received data is processed similar to the bitstream data, and the reconstructed images are displayed along with their data rates.

Fig. 7 represents the output for image transmission. The combined data rate consistently exceeds that of individual receivers, showing our algorithms perform well even on larger

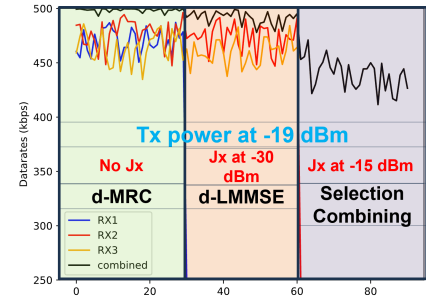


Fig. 7: Data rates for images data for indoor testbed.

datasets like images. The displayed images also demonstrate that not only is the data rate improved, but the overall quality of the received image is enhanced as well.

We transmit data at a constant power of -19 dBm. With no interference, all three receivers have similar performance along with high data rates, suggesting that d-MRC algorithm was implemented. We then introduce an external interference with power -30 dBm and notice that the receiver closest to the interference antenna, RX1 is impacted and doesn't receive good data, thus, d-LMMSE is implemented. We further increase the interference power to -15 dBm and notice that the two receivers closer to the external interference antenna are heavily impacted, leaving only RX3 to receive valid data and have higher BER than the threshold, thus, SC gets implemented with data rate matching the data rate of RX3.

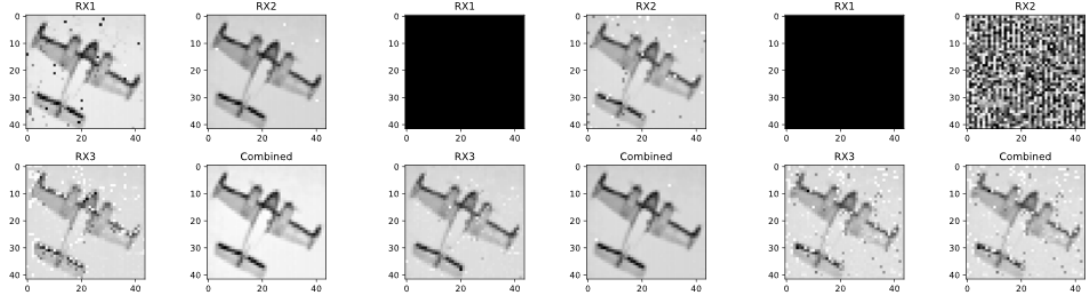
Fig. 8a - Fig. 8c are the sample reconstructed images at the receivers, displayed for each of the three cases. The figures clearly illustrate the RASHND resilience. Fig. 8a is the output for d-MRC implementation with all the RXs receiving high quality data. Fig. 8b represents d-LMMSE implementation and shows that RX1 is highly impacted, with no useful information and the combined image is the improvised version of RX2 and RX3. Fig. 8c illustrates the output for SC with RX1 and RX2 being heavily impacted. The combined image utilizes the best RX, which here is RX3.

B. Self-Healing on Outdoor Testbed

We further verify the algorithms through outdoor field tests.

1) *Results for Bitstream Data:* Similar to the indoor testbed, we first perform experiments for bitstream data by continuously transmitting with a transmit power of 1 dBm. We start with no interference case where d-MRC algorithm gets implemented. We then introduce a constant -6 dBm interference, which impacts RX1 and thus d-LMMSE is implemented. A further increase in the interference level to 4 dBm impacts both RX1 and RX2 and thus SC is implemented with the data rates being equal to that of the best RX, which here is RX3 as shown in Fig. 9.

2) *Results for Image Data:* Outdoor experiments for images are performed same as before where data is continuously transmitted with a transmit power of 1 dBm. We begin with no interference case where d-MRC algorithm gets implemented.



(a) Image for d-MRC Combining

(b) Image for d-Lmmse Combining

(c) Image for Selection Combining

Fig. 8: Received images for indoor testbed

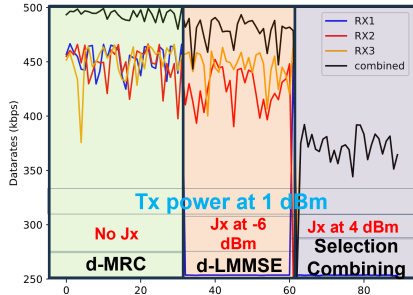


Fig. 9: Data rates for bitstream data for outdoor testbed.

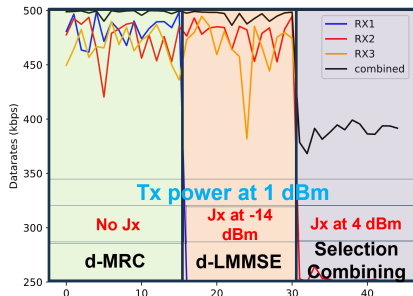


Fig. 10: Data rates for images data for outdoor testbed.

Introducing a constant interference of -14 dBm heavily impacts RX1 and thus d-LMMSE gets implemented. An increase in the interference level to 4 dBm impacts both RX1 and RX2, leading to the implementation of SC. Fig. 10 represents the continuous plot for image data through self-healing.

Fig. 11a - Fig. 11c are the sample reconstructed images at the receivers, displayed for each of the three cases. The results represent a robust prototype system. Fig. 11a is the output for d-MRC implementation with all the RXs receiving high quality data. Fig. 11b represents d-LMMSE implementation, clearly showing RX1 is highly impacted and the combined image is the improvised version of RX2 and RX3. Fig. 11c shows SC where RX1 and RX2 are heavily impacted. The

combined image selects the best RX, which here is RX3.

C. Field Test using AERPAW

The AERPAW testbed at NC State enables experimental research in a real-world outdoor environment. We leverage this testbed to transmit and receive data, which is then processed offline using our algorithms to ensure that our system is capable of providing good results when implemented in the real outdoor environment. Through these experiments, we demonstrate that our algorithms inherently accounts for and effectively mitigates challenges such as doppler shifts and dynamic channel variations, proving the robustness of our RASHND system in practical scenarios. The experiment is performed on a 1×2 SIMO setup with two moving UAVs acting as receivers and a fixed transmitter. Fig. 13 shows the path taken by the UAVs. We collect three sets of data, first one is for UAV1 taking path1 and UAV2 taking path2. For the second set, data is taken when both UAVs take path1 and the third set is for both the UAVs moving in path2. For all three cases, UAV1 is at a height of 50 m and UAV2 is at 60 m, they move at a speed of 5 m/s and have a 25 dB gain. The TX is fixed at a height of 9.144 m and has a gain of 72.5 dB. The experiments are conducted with a centre frequency of 3.32 GHz and a bandwidth of 1 MHz.

Fig. 12a - 12c shows the individual data rates and d-MRC results for all the three cases described above. It can be seen that the combined results are better than the individual data rates. Each point in x-axis corresponds to the average data rate for 500 messages and y-axis is the data rates in Kbps. The dotted lines are the average over the entire range.

VI. CONCLUSION

This paper introduces a resilient self-healing network architecture transitioning between the d-MRC, d-LMMSE and SC algorithms to obtain superior data rate values compared to the individual receivers across diverse environments in distributed SIMO systems. We evaluate the performance on bitstream and image data and show that the RASHND self-healing algorithm has superior performance in various environments. RASHND effectively uses D2D communication to share data among the devices demonstrating IDL capabilities. We validate the working of our algorithms in the real-world outdoor

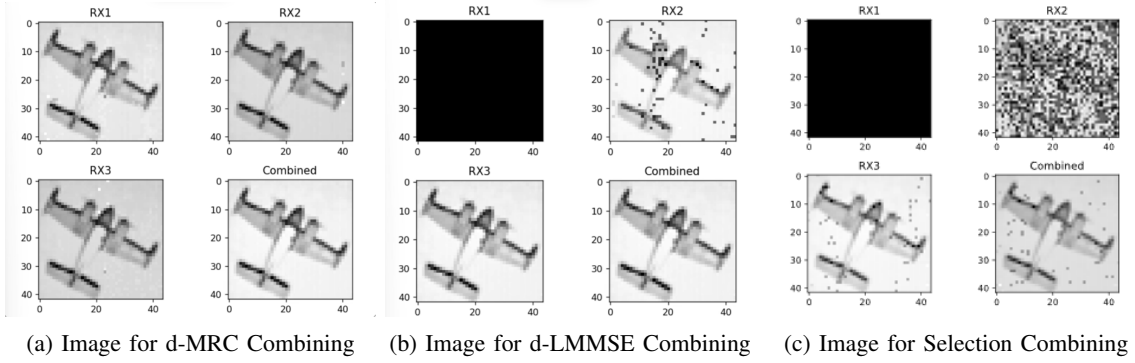


Fig. 11: Received images for outdoor testbed.

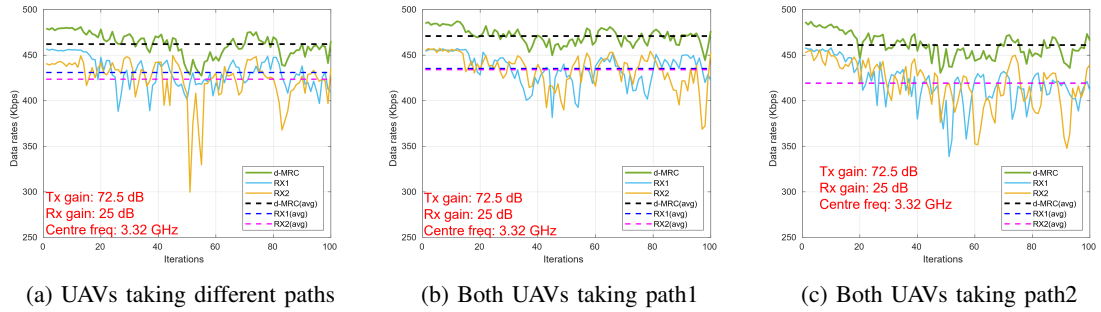


Fig. 12: Data rates for individual radios and d-MRC

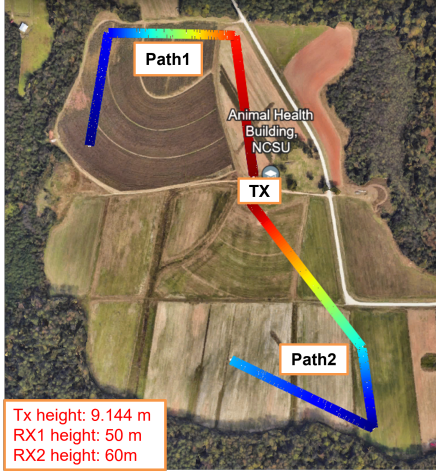


Fig. 13: Path for AERPAW experiments.

environment and also using the AERPAW testbed to emulate UAV performance. We show that the combined data rates are superior than the individual data rates for all the cases.

REFERENCES

- [1] E. Yaacoub and M.-S. Alouini, "A key 6g challenge and opportunity—connecting the base of the pyramid: A survey on rural connectivity," *Proceedings of the IEEE*, vol. 108, no. 4, pp. 533–582, 2020.
- [2] M. Mozaffari, A. Taleb Zadeh Kasgari, W. Saad, M. Bennis, and M. Debbah, "Beyond 5g with uavs: Foundations of a 3d wireless cellular network," *IEEE Transactions on Wireless Communications*, vol. 18, no. 1, pp. 357–372, 2019.
- [3] M. Giordani and M. Zorzi, "Non-terrestrial networks in the 6g era: Challenges and opportunities," *IEEE Network*, vol. 35, no. 2, pp. 244–251, 2021.
- [4] M. M. Azari, S. Solanki, S. Chatzinotas, O. Kodheli, H. Sallouha, A. Colpaert, J. F. Mendoza Montoya, S. Pollin, A. Haqiqatnejad, A. Mostaani, E. Lagunas, and B. Ottersten, "Evolution of non-terrestrial networks from 5g to 6g: A survey," *IEEE Communications Surveys & Tutorials*, vol. 24, no. 4, pp. 2633–2672, 2022.
- [5] Y. Zeng, R. Zhang, and T. J. Lim, "Wireless communications with unmanned aerial vehicles: opportunities and challenges," *IEEE Communications Magazine*, vol. 54, no. 5, pp. 36–42, 2016.
- [6] V. S. R. Kantheti, C.-H. Lin, S.-C. Lin, and L. C. Chu, "Anti-jamming resilient leo satellite swarms," in *MILCOM 2023 - 2023 IEEE Military Communications Conference (MILCOM)*, 2023, pp. 77–82.
- [7] R. Barco, P. Lazaro, and P. Munoz, "A unified framework for self-healing in wireless networks," *IEEE Communications Magazine*, vol. 50, no. 12, pp. 134–142, 2012.
- [8] M. Campion, P. Ranganathan, and S. Faruque, "A review and future directions of uav swarm communication architectures," in *2018 IEEE international conference on electro/information technology (EIT)*. IEEE, 2018, pp. 0903–0908.
- [9] M. M. Azari, G. Geraci, A. Garcia-Rodriguez, and S. Pollin, "Uav-to-uav communications in cellular networks," *IEEE Transactions on Wireless Communications*, vol. 19, no. 9, pp. 6130–6144, 2020.
- [10] V. Marojevic, I. Guvenc, R. Dutta, M. L. Sichitiu, and B. A. Floyd, "Advanced wireless for unmanned aerial systems: 5g standardization, research challenges, and aeropaw architecture," *IEEE Vehicular Technology Magazine*, vol. 15, no. 2, pp. 22–30, 2020.
- [11] R. W. Heath Jr, *Introduction to wireless digital communication: A signal processing perspective*. Prentice Hall, 2017.
- [12] D. G. Brennan, "Linear diversity combining techniques," *Proceedings of the IRE*, vol. 47, no. 6, pp. 1075–1102, 1959.
- [13] Sambrama, V. S. R. Kantheti, S.-C. Lin, L. C. Chu, and E. Blasch, "Hardware-in-the-loop implementation of distributed sdr systems and throughput-optimal coordinated transmissions," in *Proceedings of the IEEE DySPAN Workshop*, May 2024.